Mid-infrared long-baseline interferometry of the symbiotic Mira star RX Pup with the VLTI/MIDI instrument

T. Driebe [(1)], K.-H. Hofmann [(1)], K. Ohnaka [(1)], D. Schertl [(1)], and G. Weigelt [(1)]

(1) Max-Planck-Institut für Radioastronomie, Bonn, Germany

Abstract

We present mid-infrared long-baseline interferometric observations of the symbiotic Mira star RX Pup obtained with the VLTI/MIDI instrument within the framework of the Science Demonstration Time (SDT) program in February 2004. Four visibility measurements have been carried out using the unit telescopes UT2 and UT3, with projected baseline lengths ranging from 34.7 to 46.5 m. All visibility measurements show a distinct wavelength dependence: A rather steep decrease between 8 and 10 μm, and a shallower monotonic increase longward of 10 μm. For the corresponding uniform disk diameter, this visibility shape translates into a diameter increase by a factor of 2 from 25 to 50 mas between 8 and 10 μm and an almost wavelength independent diameter between 10 and 13 μm. As we show by means of radiative transfer modeling with the code DUSTY, this wavelength dependence measured with VLTI/MIDI can be interpreted as the mid-infrared signature of a circumstellar dust shell which is dominated by silicate dust.

Introduction

RX Pup belongs to the class of so-called symbiotic Miras (see, e.g.,Belczyński et al. 2000). These objects are interacting binary stars with a Mira star as primary component and a hot compact component, presumably a white dwarf, as secondary component. While the optical, UV, and X-ray part of the spectrum are dominated by emission from the hot component, the infrared regime of the SED is governed by the cool Mira star.

RX Pup is a member of the class of so-called D-type symbiotic Miras where the infrared excess seen in the SED indicates the presence of a circumstellar dust shell. Currently, ∼30 of these objects are known. RX Pup is located at a distance of $\sim 1.8\,\mathrm{kpc}$ and, as illustrated in Fig. 1, exhibited strong brightness changes in the visual and infrared regime during the last decades with a remarkable overall decline in the near-infrared brightness over the last 30 years. It is believed that these strong, nova-like brightness changes are related to unstable mass transfer to the compact companion while the small-scale modulation seen in the infrared light curves (see right panel of Fig. 1) can be attributed to the $P = 578$ d pulsation of the Mira variable. For a further discussion on RX Pup we refer to the recent detailed paper by Mikolajewska et al. (1999) and references therein. The observations of RX Pup presented here are a first step to study in detail the similarities and/or possible differences of the circumstellar environment of symbiotic and single-star Miras with dusty envelopes with the current VLTI instruments.

Observations

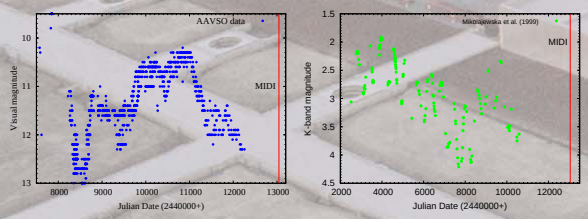

Figure 1: Visual (left) and K-band light curve (right) of RX Pup: The blue dots in the visual light curve are validated data from the AAVSO database (see http://www.aavso.org), while the dots in the K-band light curve are taken from Mikolajewska et al. (1999). In both panels the vertical red line indicates the date of the VLTI/MIDI observations. As the figure shows, at the time of the MIDI observations the symbiotic Mira RX Pup was in a phase of declining visual and NIR brightness with $M_\mathrm{V} \approx 13^\mathrm{m}$ (in line with yet unvalidated AAVSO data) and $K \approx 4^\mathrm{m}$. Taking the K-band light curve and the pulsation period $P = 578$ d determined by Mikolajewska et al. (1999) we find that the Mira component of RX Pup was close to minimum phase at the time of the MIDI observations ($\Phi_\mathrm{MIDI} \approx 0.55$).

RX Pup was observed with MIDI on three consecutive nights in February 2004 within the framework of the Science Demonstration Time (SDT) program. Interferometric data were taken with a beam combiner, which produces two interferometric signals of opposite sign, and in high sensitivity mode, i.e. the photometric data were taken after the interferometric data. A prism with a spectral resolution of $\lambda/\Delta\lambda \simeq 30$ was used to obtain spectrally dispersed fringes. The fringes were scanned by applying rapid internal optical path difference (OPD) changes of a few wavelengths around the point of zero OPD. Photometric calibration data were recorded by blocking each of the two beams alternately, immediately after recording the interferometric data. Chopping was applied in recording the photometric data to obtain sky frames (chopping parameters: ∼0.25 seconds on the target, corresponding to ∼12 target frames, followed by ∼0.25 seconds on the sky; this sequence was repeated ∼75–110 times). No chopping was performed during the recording of the interferometric data. A more detailed description of the general observing strategy is given in Leinert et al. (2004).

In total, four observations were carried out using the 89 m baseline between the unit telescopes UT2 and UT3. Due to projection effects, the projected baseline lengths range between 34.7 and 46.5 m, as can be seen in Tab. 1, where details of the individual observing runs are summarized. Calibrator stars whose angular diameter is known were observed for the calibration of the raw visibilities. Tab. 2 gives an overview of these calibration stars, their uniform-disk diameters, and the MIDI SDT observations that we used for the calibration of the raw visibilities of RX Pup.

#	Date	MJD	t_obs [UTC]	B_p [m]	P.A. [°]
1	2004 Feb 09	53045.286	06:52:08.000	34.69	63.07
2	2004 Feb 10	53046.087	02:05:54.000	46.54	28.53
3	2004 Feb 10	53046.214	05:07:37.000	41.93	52.87
4	2004 Feb 11	53047.216	05:11:39.000	41.50	53.76

Tab. 1: Summary of the VLTI/MIDI observations of RX Pup: date of observation, modified Julian date MJD, time of observation, projected baseline length B_p, and baseline projection angle P.A.

Calibrator HD number	d_UD [mas]	Date	t_obs [UTC]	MJD
18322	2.50 ± 0.12	2004 Feb 09	00:39:11.000	53045.03
		2004 Feb 09	01:39:04.000	53045.07
49161	2.88 ± 0.17	2004 Feb 09	02:45:52.000	53045.12
		2004 Feb 10	04:43:21.075	53046.20
67582	2.69 ± 0.25	2004 Feb 09	06:24:15.000	53045.27
		2004 Feb 09	07:13:39.075	53045.30
		2004 Feb 10	02:37:04.000	53046.11
		2004 Feb 10	03:46:12.000	53046.16
107446	4.54 ± 0.23	2004 Feb 09	08:08:53.000	53045.34
		2004 Feb 10	08:16:44.000	53046.34
85951	3.48 ± 0.18	2004 Feb 11	02:42:15.000	53047.11
		2004 Feb 11	05:37:52.000	53047.23
120404	3.03 ± 0.24	2004 Feb 11	07:36:34.000	53047.32
		2004 Feb 11	08:27:38.000	53047.35

Tab. 2: Summary of the VLTI/MIDI calibrator observations: HD number, uniform disk (UD) diameter, date of observation, time of observation, modified Julian date. Calibrator diameters were taken from Richichi et al. (2005).

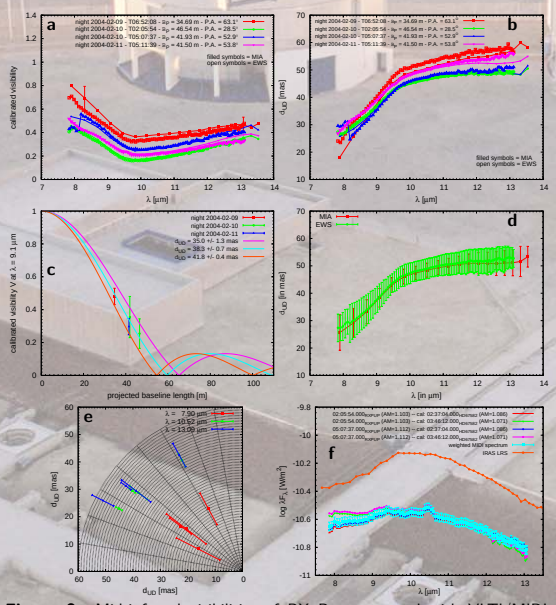

Figure 2: Mid-infrared visibilities of RX Pup measured with VLTI/MIDI in P72. (**a**): Wavelength dependence of the visibilities of RX Pup as obtained with VLTI/MIDI. The 4 measurements have been carried out with projected baselines and position angels as given in the labels. Filled symbols belong to data obtained with the MIA data reduction package (Leinert et al. 2004), whereas the open symbols give the values obtained with the EWS package (Jaffe et al. 2004). (**b**): Wavelength dependence of the apparent size of RX Pup in the mid-infrared obtained from uniform disk fits of the visibility curves shown in panel a. As the figure illustrates, the apparent diameter increases by a factor of ∼2 between 8 and 10 μm and remains roughly constant longward of 10 μm (see also next Sect.). (**c**): Simultaneous uniform disk fit of all four MIDI measurements, exemplarily shown for the MIDI data at $\lambda = 9.1\,\mu$m. (**d**): Same as panel b, but with diameters derived from simultaneous fits of all MIDI data sets as shown in panel c. The figure nicely illustrates the excellent agreement between the results obtained with the MIA and EWS data reduction packages. (**e**): Polar diagram showing the apparent diameter as a function of position angle. The accuracy of the measurements and the rather poor position angle coverage did not allow for a study of possible asymmetric structures of the dust shell. (**f**): The figure shows a comparison between the IRAS LRS (orange bullets) and 4 calibrated spectra obtained with VLTI/MIDI. The labels denote the individual calibrators used for the spectrum calibration (AM gives the airmass). Absolutely calibrated spectra for the calibrators have been taken from Cohen et al. (1999). The curve with the error bars (light blue filles squares) is the averaged MIDI spectrum of the four individual spectra weighted with the difference in airmass between calibrator and object observations. The global lower flux level of the MIDI spectra (difference of 0.2 dex) is most likely not an instrumental effect, but could probably be attributed to the overall brightness decline of RX Pup in the infrared during the last 2 decades.

Modeling

We performed 1D-radiative transfer calculations using the code DUSTY (Ivezić & Elitzur 1995) to simultaneously model the wavelength dependence of the visibility across the N band and the mid-infrared spectrum of RX Pup as it has been observed with VLTI/MIDI. We found that the results of the VLTI/MIDI observations can be best reproduced with the following model: The Mira star has $L \approx 6045\,L_\odot$, $T_\mathrm{eff} = 2500\,\mathrm{K}$, and $R = 414\,R_\odot \approx 2\,\mathrm{AU} = 1.07\,\mathrm{mas}$ (assuming a distance of 1.8 kpc). The central star is surrounded by a dust shell whose inner boundary is located at $R_\mathrm{in} = 12AU = 6 \cdot R_\star = 6.39\,\mathrm{mas}$. The dust density distribution follows a $1/r^2$ radial dependence, and best agreement with the observations is achieved when using the warm silicates from Ossenkopf et al. (1992) with a temperature at the inner dust shell boundary of 1000 K, and a grain size distribution $n \propto r^{-3.5}$ according to Mathis et al. (1977) with a maximum grain size of $0.125\,\mu\mathrm{m}$. Assuming a typical outflow velocity $v = 15\,\mathrm{km/s}$, the mass-loss rate of the Mira star can be estimated to be $\dot{M} = 2.8 \cdot 10^{-6} M_\odot/\mathrm{yr}$.

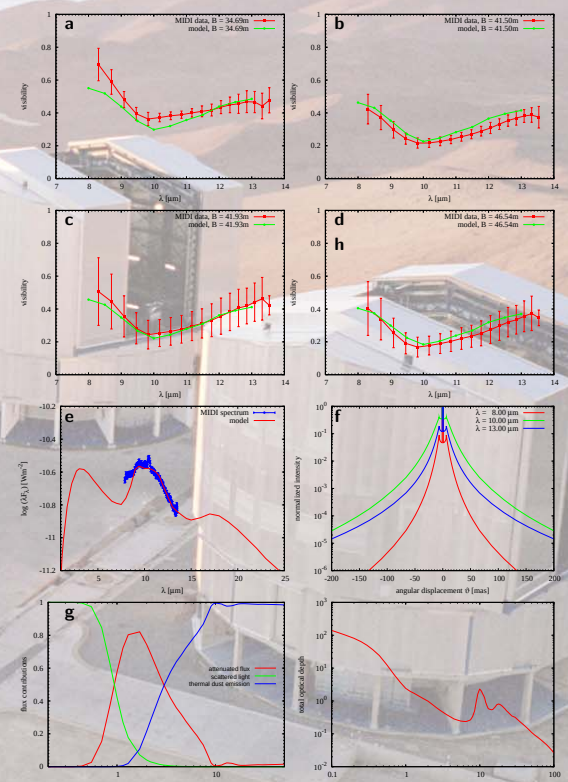

Figure 3: Modeling results and comparison with VLTI/MIDI measurements: **a-d**: Comparison of the four MIDI N-band visibility measurements of RX Pup (filled red dots with errorbars) with our currently best fitting model (green curves). Apart from some smaller deviations in the lower N-band regime at the shortest baseline (panel a) we found good agreement between model and observations. **e**: Comparison of the averaged MIDI N-band spectrum (blue bullets with errorbars) and our model spectrum (red curve). As the panel shows, the agreement is satisfactory except for the part shortward of $\sim 9\,\mu$m. **f**: Model intensity profiles at 8, 10, and $13\,\mu$m as a function of angular displacement. In all curves, the limb-brightening at the inner dust shell boundary R_in is clearly visible. From our model, we find $R_\mathrm{in} \approx 6 \cdot R_\star$. **g**: Contributions from the attenuated central star flux, scattered light emission, and thermal dust emission as a function of wavelength. As the panel shows, the contribution of thermal dust emission increases from $\sim 90\%$ to $\sim 100\%$ between 8 and 10 μm, which, apart from the optical depth changes, is responsible for the observed steep visibility drop in this wavelength regime (see panels a-d). **h**: Total optical depth as a function of wavelength for the silicate chemisty of Ossenkopf et al. (1992) used in the present modeling. Due to the silicate feature, the optical depth rises from ~ 0.3 at $8\,\mu$m to 2.3 at $10\,\mu$m, before it drops again to reach ~ 0.6 at $13\,\mu$m.

References

- Belczyński, K., Mikolajewska, J., Munari, U., et al. 2000, *Astr. Astrophys. Suppl.* **146**, 407
- Cohen, M., Walker, R. G., Carter, B., et al. 1999, *Astron. J.* **117**, 1864
- Ivezić, Z., Elitzur, M. 1995, *ApJ* **445**, 415
- Jaffe, W., Meisenheimer, K., Röttgering, H. J. A., et al. 2004, *Nature* **429**, 47
- Leinert, Ch., van Boekel, R., Waters, L. B. F. M., et al. 2004, *A&A* **423**, 537
- Mathis, J. S., Rumpl, W., Nordsieck, K.H. 1977, *ApJ* **217**, 425
- Mikolajewska, J., Brandi, E., Hack, W., et al. 1999, *MNRAS* **305**, 190
- Ossenkopf, V., Henning, Th., Mathis, J. S. 1992, *A&A* **261**, 567
- Richichi, A., Percheron, I., Khristoforova, M. 2005, *A&A* **431**, 773

Poster presented at the ESO workshop
The power of optical/IR interferometry: recent scientific results and 2nd generation VLTI instrumentation
4th-8th April 2005, Garching, Germany
contact e-mail: driebe@mpifr-bonn.mpg.de